1-1-2009

Optimization of Electrostatically Actuated Miniature Compressors for Electronics Cooling

A. A. Sathe

E. A. Groll
Purdue University

S. V. Garimella
Purdue University

available at www.sciencedirect.com

ScienceDirect

journal homepage: www.elsevier.com/locate/ijrefrig

Optimization of electrostatically actuated miniature compressors for electronics cooling

Abhijit A. Sathe, Eckhard A. Groll, Suresh V. Garimella*

NSF Cooling Technologies Research Center, School of Mechanical Engineering, Purdue University, 585 Purdue Mall, West Lafayette, IN 47907, USA

ARTICLE INFO

Article history:
Received 12 June 2008
Received in revised form
30 March 2009
Accepted 7 April 2009
Published online 17 April 2009

Keywords:
Refrigeration system
Compression system
Cooling
Component
Electronic
Optimization
Design
Compressor

ABSTRACT

This paper explores the feasibility of using electrostatically actuated diaphragm compressors in a miniature-scale refrigeration system for electronics cooling. A previously developed experimentally validated analytical model for the diaphragm compressor is used in conjunction with an optimization approach to determine the required dimensions for the compressor. The analysis reveals that the pressure rise and volume flow rate required for the electronics cooling application are not achieved using a single compressor because of material property limitations. A three-dimensional array of compressors is proposed instead with which the cooling requirements and the size restrictions for electronics cooling applications may be simultaneously satisfied.

Optimisation de compresseurs miniaturisés à commande électrostatique utilisés pour refroidir les systèmes électroniques

Mots clés : Système frigorifique ; Système à compression ; Refroidissement ; Composant ; Électronique ; Optimisation ; Conception ; Compresseur

* *Corresponding author.*
E-mail address: groll@purdue.edu (E.A. Groll).
0140-7007/$ – see front matter
doi:10.1016/j.ijrefrig.2009.04.001

Nomenclature

AR	chamber aspect ratio, (R/Y)
COP	coefficient of performance
D	applied DC voltage (V)
E	elastic modulus of diaphragm (GPa)
Freq	diaphragm actuation frequency (Hz)
M	number of compressors in series
N	number of compressors in parallel
n	polytropic compression index
R	chamber radius (mm)
R_1	chamber radius for first optimization parameter
R_2	chamber radius for second optimization parameter
$\overline{R}$	specific gas constant ($J\,kg^{-1}\,K^{-1}$)
T	temperature (K)
$\dot{V}$	volume flow rate ($ml\,min^{-1}$)
Vol	volume (cm^3)
υ	refrigerant specific volume ($m^3\,kg^{-1}$)
$\dot{W}_{ther}$	theoretical compression work (mW)
w	diaphragm thickness (μm)
Y	maximum chamber depth (μm)

Greeks

β	diaphragm Poisson's ratio
σ	initial stress in diaphragm (MPa)
ΔP	pressure rise in the chamber (kPa)
η_{Vol}	volumetric efficiency of compressor

Subscripts

dis	discharge
suc	suction
ther	thermal

1. Introduction

With the rapid trend towards higher performance and ultra-compact form factors for portable computers, and the steady increase in heat generation in the CPUs, GPUs, memory modules and disk drives, heat dissipation in electronic systems has become even more challenging. Traditional electronics cooling approaches such as forced convective air cooling using conventional heat sinks are soon expected to reach their limits for meeting the dissipation needs of these emerging high-performance electronics' systems (Krishnan et al., 2007). Alternative electronics cooling approaches include heat pipes, liquid immersion, jet impingement and sprays, microchannel heat sinks, thermoelectric cooling, and refrigeration (Garimella, 2006). Vapor compression refrigeration appears to be among the more promising techniques because of its ability to operate at varying loads and high ambient temperatures. A schematic representation of a vapor compression refrigeration system for electronics cooling is shown in Fig. 1. The advantages of refrigeration cooling over conventional techniques are (Phelan, 2001): (a) maintenance of low junction temperatures while dissipating high heat fluxes, (b) potential increase in microprocessor performance at lower operating temperatures, and (c) increased chip reliability. However, these advantages must be balanced against the following drawbacks: (a) increased complexity and cost of the cooling system, (b) a possible increase in cooling system volume, and (b) uncertainties in the system reliability due to the moving parts in the compressor.

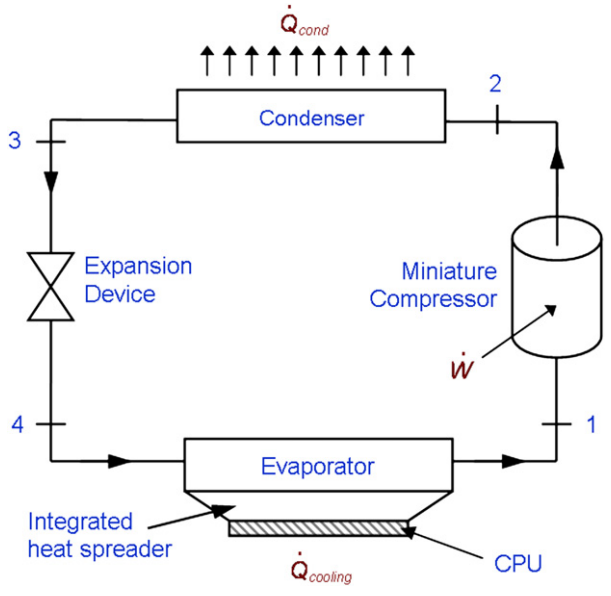

Fig. 1 – Schematic representation of a miniature refrigeration system for electronics cooling.

Over the past few years, several researchers have investigated the feasibility of using miniature-scale vapor compression refrigeration systems for microprocessor cooling. A vapor compression system model for electronics cooling based on thermodynamic and heat transfer considerations was developed by Bash (2001). Cycle components were analyzed by combining the principles of thermodynamics and heat transfer in order to account for irreversibilities inherent in practical systems. A conventional vapor compression system, consisting of a serpentine evaporator, an intercooler, a compressor, a plate fin-and-tube condenser, and a capillary tube expansion device, was tested. The modeling results were validated against the experimental results with the COP predictions matching within ±8% for heat loads between 210 and 400 W.

Bash et al. (2002) discussed a vapor compression system for cooling of microprocessor chips and identified a need for capacity control of the compressor to account for thermal load variations in the system. They proposed, built and tested a variable capacity acoustic compressor and showed that the refrigeration cycle could handle a load variation from 20% to 100% while maintaining a reasonable COP.

Heydari (2002) developed a steady-state simulation model of a refrigeration cycle for cooling of computers based on four sub-models of the cooling system consisting of a free-piston

linear compressor, a compact condenser, a capillary tube, and a cold plate evaporator. The model was based on a simple thermodynamic control volume approach and semi-empirical mass flow rate correlations for capillary tubes. It also used a lumped method to calculate the heat transfer rate and empirical correlations to estimate the pressure drop in the condenser.

Mongia et al. (2006) developed one of the first miniature refrigeration systems for cooling of high-power components in a notebook computer. Their system employed small component prototypes specifically designed for a notebook form factor, including a microchannel condenser, a microchannel cold plate evaporator, and a miniature-scale linear piston compressor. Isobutane was used as the refrigerant for the prototype system, which achieved a cooling rate of approximately 50 W and a system COP of approximately 2.25. The overall isentropic efficiency of the linear compressor was measured to be in the range of 33–35%. Information on the reliability of the linear compressor was not provided. A simulation model for analysis and optimization of the compressor or the refrigeration cycle was also not developed.

The feasibility and potential of miniature vapor compression refrigeration systems for electronics cooling were explored by Cremaschi et al. (2007). A detailed review of recent small-scale refrigeration systems along with their performance potential and challenges was discussed. The authors concluded that efficient and reliable mini- and micro-compressors are essential in order to achieve energy efficiencies that would render refrigeration systems competitive with other electronics cooling technologies.

Trutassanawin et al. (2006) experimentally tested a small-scale refrigeration system consisting of a commercially available miniature-scale compressor, a microchannel condenser and a cold plate evaporator. The system achieved a maximum cooling capacity of 226 W while maintaining the maximum CPU temperature at 53 °C. The system performance was found to strongly depend on the compressor efficiency. The overall isentropic and volumetric efficiencies of this compressor, which was not designed for electronics cooling applications, were as low as 25% and 50%, respectively, which is well below typical efficiencies for conventional compressors. It was argued that COP improvements of 5–18% could be reached if a well-designed compressor was used. The experimental measurements did not compare very well with the simulation model (Trutassanawin, 2006), with the deviations attributed to the unavailability of a correlation for accurately predicting the quality-based heat transfer coefficient in the cold plate microchannel heat sink for refrigerant boiling heat transfer. It was recommended that more accurate correlations to predict the refrigerant flow boiling heat transfer coefficient and better designs of miniature compressors targeted specifically for electronics cooling are needed to improve the system performance. While Bertsch et al. (2008) have attempted to address the former recommendation, the present work discusses development and optimization of a miniature compressor.

The maximum dimensions, possible compressor shapes, and their respective physical volumes chosen based on industry recommendations (ITRS, 2006) for an 80 W laptop computer cooling application are shown in Fig. 2. Compressors of this size as part of a refrigeration system can be

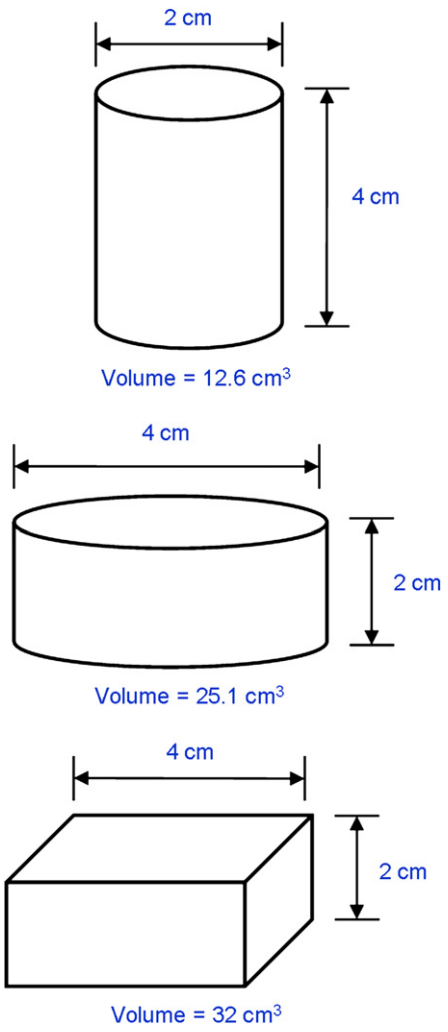

Fig. 2 – Possible compressor shapes and dimensions for an 80 W laptop computer cooling application.

Table 1 – Design parameters for the miniature refrigeration system using three refrigerants.

Requirements			
System cooling capacity	80 W	–	–
Evaporator temperature	20 °C	–	–
Suction superheat	5 K	–	–
Condenser temperature	35 °C	–	–
Condenser subcooling	5 K	–	–
Compressor overall isentropic efficiency[a]	65%	–	–
Compressor volumetric efficiency[a]	90%	–	–
Calculations	**R134a**	**R236fa**	**R245fa**
Suction pressure, kPa	572	230	124
Discharge pressure, kPa	888	376	213
Pressure rise (ΔP_{net}), kPa	316	146	89
Volume flow rate ($\dot{V}_{net}$), ml min^{-1}	1141	2496	4119
Theoretical COP	12.0	12.3	12.4

a Assumed for this analysis.

accommodated inside the form factor of a laptop computer. Performance requirements and design parameters for the miniature refrigeration cycle are listed in Table 1. The choice of refrigerant is critical in the design of a compressor. It determines the required pressure rise in the compressor as well as the refrigerant mass flow rate for a given cooling capacity. Moderate vapor pressure, high latent heat of vaporization, non-flammability, and low impact on the environment are among the desired properties in a refrigerant. Of the many alternatives, R134a is chosen for the present analysis, since it is well suited to the present application due to its ability to satisfy most of the desired conditions. In addition, two relatively new HFC refrigerants, namely R236fa and R245fa, which also exhibit suitable characteristics, are considered in this analysis as well. Based on a thermodynamic cycle analysis, the pressure rise and flow rate requirements for refrigeration cycles working with these three refrigerants are also listed in Table 1. Since the thermodynamic cycle for the miniature refrigeration system applicable to electronics cooling discussed here is not different from that for a conventional vapor compression system, the COP of the cycle (listed in Table 1) is identical to that of state-of-the-art systems at similar operating conditions.

Prevention of moisture condensation if the evaporator temperature drops below the ambient dew point is an important consideration. It is expected that in typical controlled environments such as office spaces, the evaporator temperature of 20 °C considered here will exceed the dew point temperature at all times. The chip temperature would be even higher because of the thermal resistances of the TIMs and the heat spreader.

An electrostatically actuated diaphragm compressor offers promise for the miniature cooling system application because of its potential for high efficiency, compactness and scalability. The diaphragm compressor, schematically represented in Fig. 3, consists of a flexible circular diaphragm clamped at its circumference, enclosed by two identical halves of a conformal chamber. Gas is admitted into the chamber through the suction ports along the circumference, while the discharge valves control discharge flow and pressure rise. Metallic electrode layers are deposited on the diaphragm and on the chamber surfaces and dielectric layers are deposited on the top of the metallic electrodes to prevent electrical shorting when the diaphragm touches the chamber surface. The principle of operation of the diaphragm compressor is based on progressive electrostatic zipping of the diaphragm towards the chamber when a DC potential difference is applied across them. An analytical model for such a diaphragm compressor was developed by the authors (Sathe et al., 2008), and validated against results from the literature as well as against experimental results conducted using a custom test setup. The diaphragm compressor model and comparisons were limited to a specific set of geometric parameters, and the effects of variation of the chamber dimensions on the overall performance of the diaphragm compressor were not considered. For a potential application in electronics cooling, an optimized design of the diaphragm compressor that offers the best performance at the lowest compression power is desired. The analytical model of Sathe et al. (2008) is used in the present work to conduct an optimization study for the diaphragm compressor.

The focus of the present study is on optimization of the electrostatic compressor design, and not that of the whole refrigeration system. Since this is a relatively new compression technology, operating issues such as leaks, reliability, instability, and noise have not been considered in this analysis.

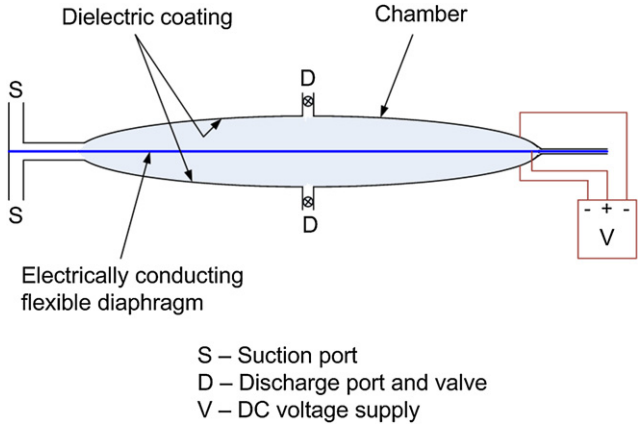

Fig. 3 – Schematic diagram of an electrostatically actuated diaphragm compressor.

2. Pressure rise vs. volume flow rate

The analytical diaphragm compressor model of Sathe et al. (2008) predicts the required pull-down voltage for achieving a specified pressure rise. While the dielectric constant of the dielectric layer on the chamber surface limits the maximum pull-down voltage that can be imposed before dielectric breakdown, the maximum pressure rise achieved in the chamber is limited by the geometric and elastic properties of the diaphragm. The diaphragm stress analysis in Sathe et al. (2008) indicates that the maximum chamber pressure rise

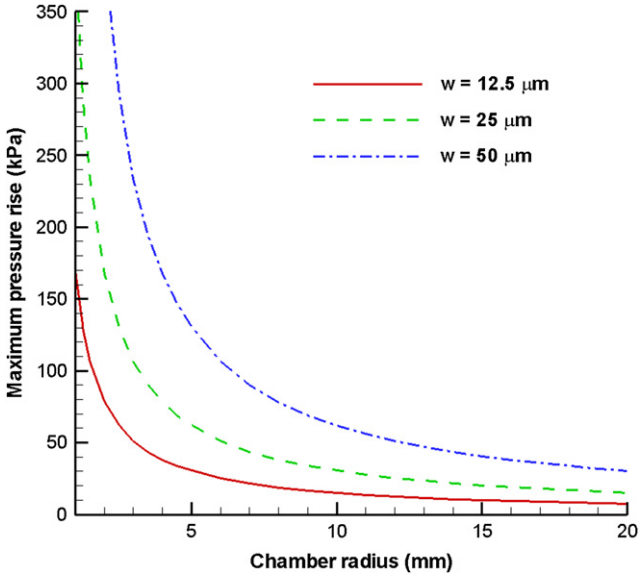

Fig. 4 – Maximum sustainable pressure rise for different radii (*R*) and thicknesses (*w*) of the Kapton diaphragm.

allowed so that the deformation of the diaphragm remains in the elastic range is given as

$$\Delta P_{max} = f(R, w, E, \beta, \sigma) \quad (1)$$

For instance, plastic deformation of a diaphragm made of DuPont Kapton beyond its elastic limit of 3% (DuPont, 2006) is irreversible and therefore undesirable. The maximum possible pressure rise in the chamber as a function of the chamber radius for a Kapton diaphragm with different thicknesses is plotted in Fig. 4. Based on the trends, the maximum sustainable pressure increases as the chamber radius decreases.

The volume flow rate of the compressor is a function of the chamber volume and the pumping frequency as shown below:

$$\dot{V} = \mathrm{Vol}_{chamber} \cdot \mathrm{Freq} \cdot \eta_{Vol} \quad (2)$$

The chamber swept volume is given as

$$\mathrm{Vol}_{chamber} = 4 \cdot \pi \cdot R^2 \cdot Y \cdot \int_0^1 y(r) \cdot r \cdot dr \quad (3)$$

where Y is the maximum depth of the chamber given in terms of the chamber radius and the aspect ratio (AR). The total chamber volume consists of the volume of both halves of the chamber. The term $y(r)$ in Eq. (3) is the non-dimensional representation of the chamber profile, r is the non-dimensional radius of the chamber ($0 \le r \le 1$) and y is the non-dimensional depth of the chamber at any radius r ($0 \le y \le 1$). Based on Eq. (3), the volume flow rate increases as the chamber radius increases.

To summarize, the compressor pressure rise and volume flow rate are related to the chamber geometry as follows:

$$\begin{matrix} \Delta P \propto \dfrac{1}{R^2} \\ \dot{V} \propto R^3 \end{matrix} \quad (4)$$

Using the design parameters described in Table 2, these variations are graphically shown in Fig. 5(a) where the chamber pressure rise and refrigerant volume flow rate are plotted as a function of the chamber radius. The inherent trade-off between the pressure rise and the flow rate is shown in Fig. 5(b). Since these two parameters may be independently controlled, it is possible to arrive at an optimal design which would maximize the performance of the compressor, as is shown in the following section.

Table 2 – Design parameters for the diaphragm compressor.

Chamber profile	Dome-shaped (Sathe et al., 2008)
Chamber aspect ratio (AR)	100
Dielectric thickness on chamber surface	1 μm
Dielectric constant	3.5
Diaphragm material	Kapton (DuPont, 2006)
Diaphragm thickness (w)	25 μm
Diaphragm elastic modulus (E)	3 GPa
Diaphragm Poisson's ratio (ν)	0.3
Diaphragm initial stress (σ)	15 MPa
Pumping frequency (Freq)	90 Hz

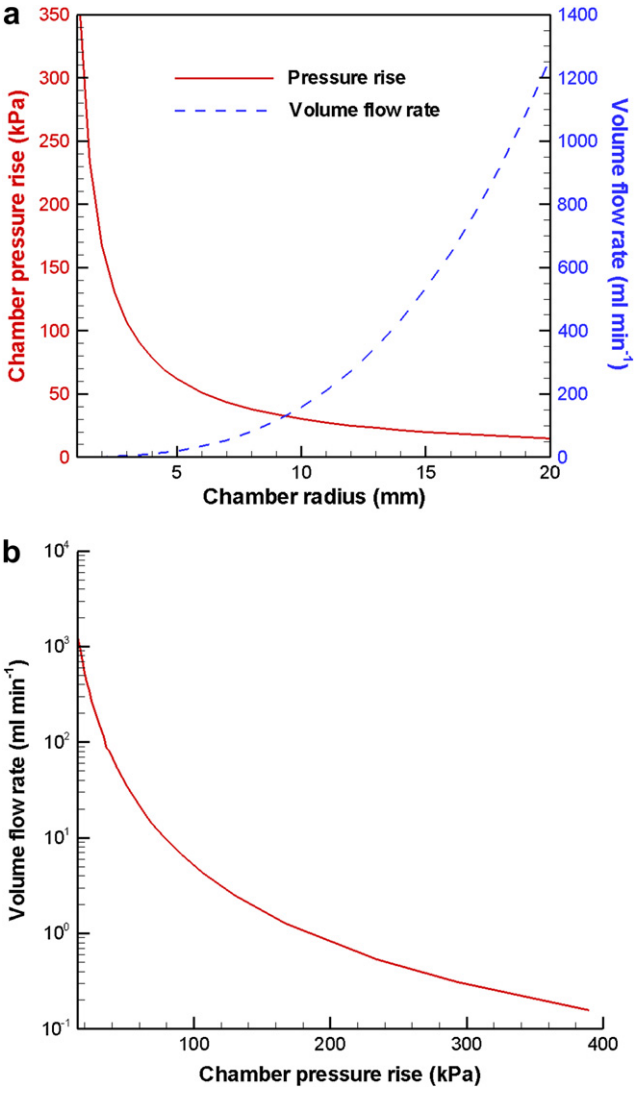

Fig. 5 – Variation of (a) chamber pressure rise and refrigerant volume flow rate with chamber radius, and (b) volume flow rate with pressure rise.

3. Compressor performance optimization

It is clear from the foregoing discussion that the optimal performance of the diaphragm compressor would be achieved with the pressure rise–volume flow rate relationship as shown in Fig. 5(b). The first optimization strategy involves minimizing the thermodynamic compression power. While this metric differs from the actual power input to the compressor, minimizing the compression power would maximize the thermodynamic efficiency of the compressor. Compression power for a polytropic compression process is given as (Moran and Shapiro, 2004):

$$\dot{W}_{ther} = \frac{n \cdot \nu_{suc} \cdot \dot{V} \cdot \overline{R} \cdot T_{suc}}{n-1} \cdot \left[1 - \left(\frac{P_{dis}}{P_{suc}} \right)^{\frac{n-1}{n}} \right] \quad (5)$$

where $n = 1.178$ and $\overline{R} = 81.49\ \mathrm{J\,kg^{-1}\,K^{-1}}$ for the refrigerant

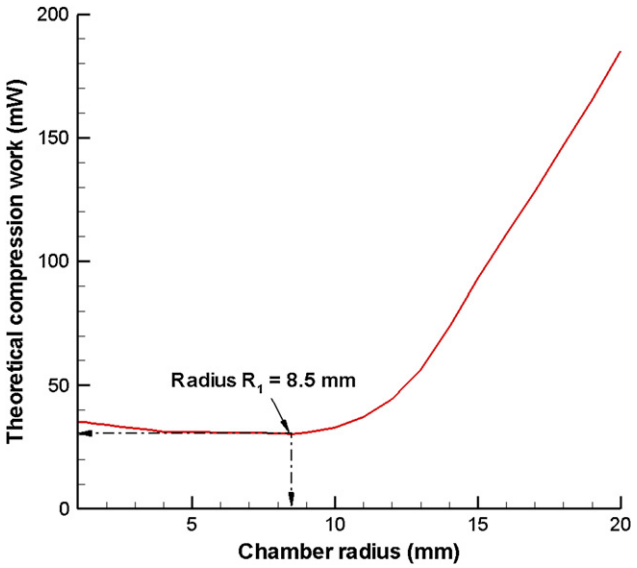

Fig. 6 – Optimization of compressor chamber dimensions for minimum theoretical compression work for refrigerant R134a (optimum chamber radius $R_1 = 8.5$ mm).

R134a. The compressor discharge pressure (P_{dis}) is the sum of the suction pressure and chamber pressure rise given as

$$P_{dis} = P_{suc} + \Delta P \quad (6)$$

Using the chamber pressure rise estimated from Fig. 5(a) in Eq. (5), the variation of the theoretical compression work with the chamber radius is plotted in Fig. 6. The compression work slightly drops as the radius of the chamber is increased. After reaching a minimum (30.1 mW), it increases rapidly with further increase in the chamber radius. The existence of a minimum reflects the trade-off discussed in Eq. (4). The

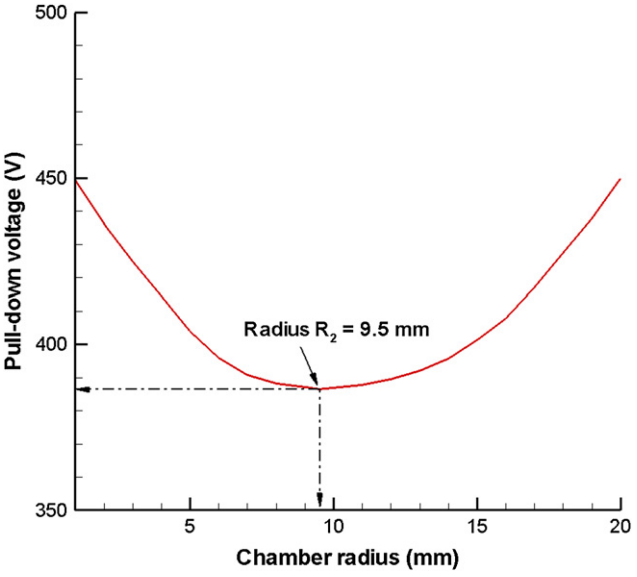

Fig. 7 – Optimization of compressor chamber dimensions for minimum pull-down voltage for refrigerant R134a (optimum chamber radius $R_2 = 9.5$ mm).

Table 3 – Design parameters for the optimized diaphragm compressor.

Chamber radius	8.5 mm
Maximum chamber depth	85 μm
Maximum pressure rise	35.6 kPa
Volume flow rate	97 ml min^{-1}
Pull-down voltage	387 V

chamber radius (R_1) corresponding to the minimum thermodynamic compression work for the selected conditions is approximately 8.5 mm. The compression power shown in Fig. 6 is the theoretical thermodynamic power, and not the actual electrical power. The diaphragm compressor power consumption is very low due to the fact that it operates under a voltage differential and only small currents are required. In previous work by the authors (Sathe et al., 2008), for a chamber radius of approximately 6 mm and an applied DC voltage of 500 V, a current of 1 mA was observed; this implies an electrical power consumption of 500 mW.

For an electrostatically actuated diaphragm compressor, another important design parameter is the required diaphragm pull-down voltage, in addition to the pressure rise and the volume flow rate. Higher operating voltages require increased dielectric layer thicknesses, and are undesirable due to difficulties in practical implementation. Based on a detailed analysis, the pull-down voltage for the given chamber geometry and pressure rise were derived in Sathe et al. (2008):

$$D \propto \frac{Y}{R} \cdot \sqrt{\Delta P} \quad (7)$$

Using a dome-shaped chamber geometry and the diaphragm and dielectric properties listed in Table 2, the pull-down voltage is calculated as a function of the chamber radius in Fig. 7. As the chamber radius is increased, the chamber depth Y also increases, which weakens the electrostatic field in the chamber. At the same time, increasing the chamber radius

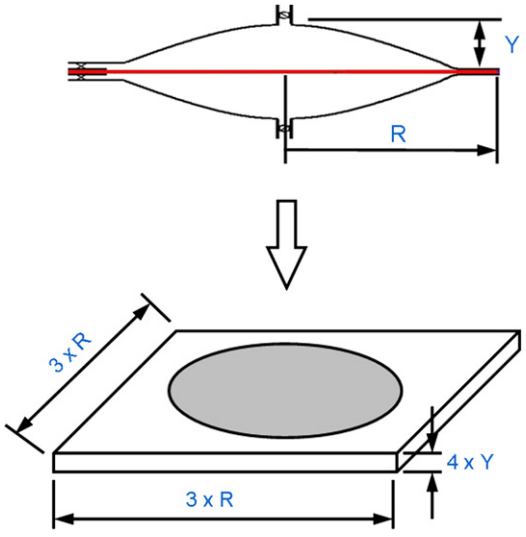

Fig. 8 – Definition of external dimensions of a diaphragm compressor unit as a function of the chamber dimensions (not to scale).

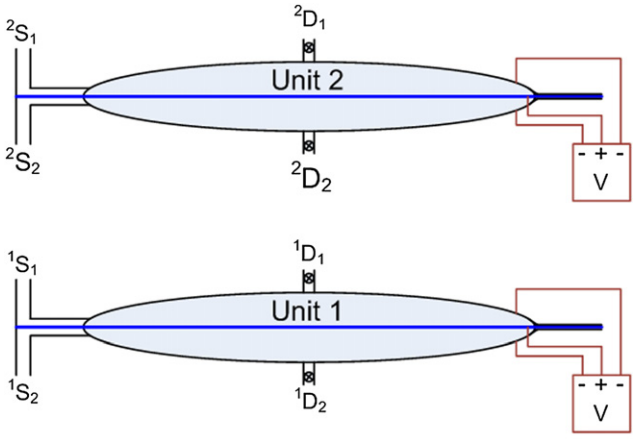

From	To
Suction manifold	$^1S_1$ and $^1S_1$
$^1D_1$	$^1S_1$
$^1D_2$	$^1S_2$
$^2D_1$ and $^2D_2$	Discharge manifold

Fig. 9 – Schematic representation of a series arrangement with two diaphragm compressor units for enhancing the refrigerant pressure rise.

increases the surface area of the diaphragm and the chamber surface, which results in an increase in the electrostatic force. As a result of these opposing effects, the pull-down voltage initially decreases, reaches a minimum and then increases with a further increase in the chamber radius. The minimum pull-down voltage (386.5 V) is realized at a chamber radius (R_2) of 9.5 mm.

The pull-down voltage for a thermodynamic compression work-based optimum radius of R_1 is 387.7 V, which is 0.3% higher than the pull-down voltage at radius R_2 for minimum pull-down voltage. On the other hand, the thermodynamic compression power at radius R_2 of 31.8 mW is 5.2% higher than that at radius R_1. Hence, radius ($R_1 = 8.5$ mm) is selected as the optimized chamber radius at which the theoretical power and the pull-down voltage are together minimized. For an aspect ratio of 100, the maximum chamber depth would be 85 μm. The different design parameters for the compressor chamber of this geometry are shown in Table 3.

Comparing the pressure rise and volume flow rate required for the 80 W laptop cooling application (Table 1) and the actual deliverable quantities (Table 3), it is clear that the cooling requirement cannot be satisfied by using a single diaphragm compressor unit. In the next section, the feasibility of constructing an array of compressor units for satisfying the cooling requirement is discussed. The analysis is conducted using three different refrigerants, R134a, R236fa and R245fa, which were determined as suitable working fluids for this application in Section 1.

4. Diaphragm compressor array

To achieve the pressure rise and refrigerant volume flow rate required for the 80 W laptop cooling application, an array of the diaphragm compressors discussed above is required, where multiple units are arranged in a series–parallel combination to achieve the desired volume flow rate and the desired pressure rise, respectively, in the available volume. This is similar to the 3-D array of dual-diaphragm pumps proposed by Cabuz et al. (1999) for enhancing the volume flow rate. The optimized chamber dimensions from the previous section are used for defining the external dimensions of an individual compressor unit as shown in Fig. 8, which shows a representative transformation of chamber dimensions into those of a complete compressor unit. The additional space allowed accounts for the manifolds, valves and electronics. The physical external volume of the compressor unit is given as

$$\mathrm{Vol}_{\mathrm{unit}} = 36 \cdot R^2 \cdot Y \tag{8}$$

In a series arrangement, the discharge of one compressor unit is passed to the suction of the other (Fig. 9). Hence, the series arrangement enhances the pressure rise obtained, as also proposed by Yoon (2006). Neglecting the pressure drop in the piping, for M compressor units in series, the net pressure rise of the arrangement is given as

$$\Delta P_{\mathrm{net}} = M \cdot \Delta P_{\mathrm{unit}} \tag{9}$$

A parallel arrangement, on the other hand, involves arranging each compressor unit such that the pressure rise achieved with each is the same, but the volume flow rate is increased (Fig. 10). The volume flow rate for an arrangement with N compressor units in parallel is given as

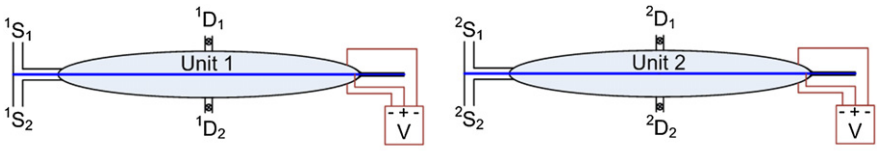

From	To
Suction manifold 1	$^1S_1$ and $^1S_1$
Suction manifold 2	$^2S_1$ and $^2S_1$
$^1D_1$ and $^1D_2$	Discharge manifold 1
$^2D_1$ and $^2D_2$	Discharge manifold 2

Fig. 10 – Schematic representation of a parallel arrangement with two diaphragm compressor units for enhancing the refrigerant volume flow rate.

Table 4 – Design parameters for the optimized diaphragm compressor using three refrigerants.

Refrigerant	R134a	R236fa	R245fa
Number of units in series (N)	16	4	3
Number of units in parallel (M)	12	26	42
Total number of units ($M \times N$)	172	104	126
External volume of single unit (Vol_{unit}), cm^3	0.221	0.221	0.221
External volume of the array (Vol_{net}), cm^3	31.84	22.98	27.85
Available external volume (Fig. 2), cm^3	32	32	32

$$\dot{V}_{net} = N \cdot \dot{V}_{unit} \tag{10}$$

The necessary pressure rise and volume flow rate for the 80 W cooling capacity (Table 1) can thus be generated using a 3-D array with M units in series and N units in parallel. The external physical volume of the array is given as

$$Vol_{net} = M \cdot N \cdot Vol_{unit} \tag{11}$$

Using Table 1, Table 3 and Eqs. (8)–(11), the number of required compressor units in series (M) and in parallel (N), and the external physical volume of the $M \times N$ array, is calculated and summarized in Table 4 and also shown graphically in Fig. 11. For the given application, 3-D compressor arrays of 172, 104 and 126 diaphragm compressors are needed to make up the required pressure rise and volume flow rate using refrigerants R134a, R236fa and R245fa, respectively. The calculated volumes of the diaphragm compressor arrays are compared with the available volume for the compressor (from Fig. 2). The comparison indicates that it is theoretically possible to fit 3-D compressor arrays using any of these refrigerants within the volume constraint of 32 cm^3. While it is not feasible to demonstrate that such an array would fit inside the *shape* of the geometry defined in Fig. 2, Fig. 11 shows that this array would fit inside the *volume* of the geometry.

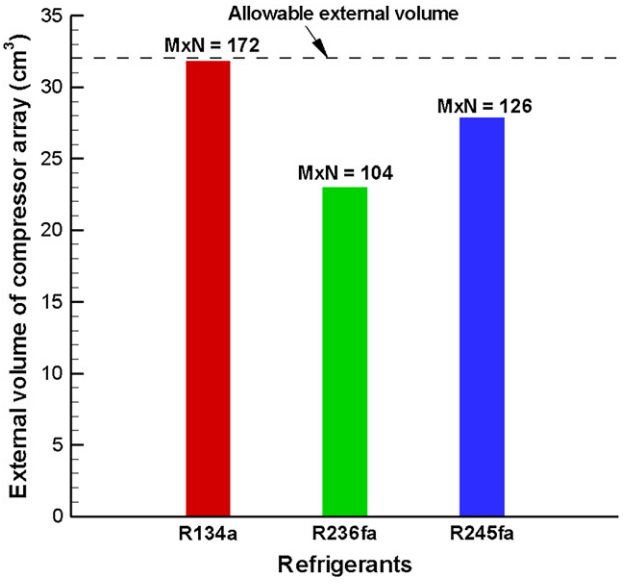

Fig. 11 – Comparison of external volumes of the compressor arrays using different refrigerants with total number of units required ($M \times N$).

While a steady heat load of 80 W is assumed for the analysis, load variation in the system can also be readily addressed. When the heat load decreases, the refrigerant mass flow rate must be correspondingly decreased. This would result in an increase in condenser pressure and in the quality of refrigerant entering the evaporator. The desired control of the mass flow rate can be achieved by adjusting the frequency of operation of the diaphragm compressor array (Eq. (2)). A change in the frequency of diaphragm actuation does not affect the operating voltage of the compressor (Sathe, 2008). Hence, capacity control of the compressor without compromising the performance for a variable load, as discussed by Bash et al. (2002), is feasible with diaphragm compressors. Synchronizing the individual compressor units to match the load variations is an operation-related issue which would need to be resolved.

5. Conclusions

An optimization procedure for use of electrostatically actuated diaphragm compressors in an electronics cooling application is presented. The maximum pressure differential achieved in the compressor is observed to be a function of the maximum strain allowable for the diaphragm before it reaches the elastic limit. A correlation between the pressure rise and the volume flow rate shows that the two are related to the chamber radius in opposing ways, i.e., increasing the chamber radius decreases the former and increases the latter. Hence, to achieve a trade-off, two different optimization strategies are analyzed: minimizing the theoretical compression work, and minimizing the required pull-down voltage for the diaphragm. The optimization leads to a given set of dimensions for the diaphragm compressor, from which the external volume occupied by a single compressor is estimated. Three different refrigerants are evaluated. Since a single compressor unit is not capable of satisfying the need desired 80 W cooling capacity, a 3-D array of diaphragm compressors is proposed. Based on the optimized dimensions, it is shown that it is possible to achieve the desired cooling using arrays of compressors within the specified volume constraint of 32 cm^3 using any of the three refrigerants.

While the fabrication complexities and associated cost for such a compressor array have not been considered in this analysis, it is believed that with rapid advances in the silicon microfabrication techniques, the diaphragm compressor holds promise for miniature refrigeration systems.

Acknowledgments

The authors acknowledge financial support for this work from members of the Cooling Technologies Research Center, a National Science Foundation Industry/University Cooperative Research Center at Purdue University.

REFERENCES

Bash, C.E., 2001. Analysis of refrigerated loops for electronics cooling. In: Proceedings of IPACK'01 – The Pacific Rim/ASME International Electronic Packaging Technical Conference and Exhibition, Kauai, Hawaii, pp. 811–819.

Bash, C.E., Patel, C.D., Beitelmal, A., 2002. Acoustic compression for the thermal management of multi-load electronic system. In: Thermomechanical Phenomena in Electronic Systems – Proceedings of the Intersociety Conference, pp. 395–402.

Bertsch, S.S., Groll, E.A., Garimella, S.V., 2008. Refrigerant flow boiling heat transfer in parallel microchannels as a function of local vapor quality. International Journal of Heat and Mass Transfer 51, 4775–4787.

Cabuz, C., Cabuz, E.I., Herb, W.R., Rolfer, T., Zook, D., 1999. Mesoscopic sampler based on 3D arrays of electrostatically actuated diaphragms. In: Proceedings of the 10th International Conference on Solid-State Sensors and Actuators, Transducers'99, Sendai, Japan, pp. 1890–1891.

Cremaschi, L., Groll, E.A., Garimella, S.V., 2007. Performance potential and challenges of future refrigeration-based electronics cooling approaches. Proceedings of THERMES 2007. Millpress, Santa Fe, New Mexico, pp. 119–128.

DuPont, Inc., 2006. DuPont Kapton HN polyimide film data sheet. http://www2.dupont.com/Kapton/en_US/assets/downloads/pdf/HN_datasheet.pdf.

Garimella, S.V., 2006. Advances in mesoscale thermal management technologies for microelectronics. Microelectronics Journal 37 (11), 1165–1185.

Heydari, A., 2002. Miniature vapor compression refrigeration systems for active cooling of high performance computers. The 8th Intersociety Conference on Thermal and Thermomechanical Phenomena in Electronic Systems (I-THERM), pp. 371–378.

International Technology Roadmap for Semiconductors, 2006. Assembly and Packaging. Semiconductor Industry Association.

Krishnan, S., Garimella, S.V., Chrysler, G.M., Mahajan, R.V., 2007. Towards a thermal Moore's law. IEEE Transactions on Advanced Packaging 30 (3), 462–474.

Mongia, R., Masahiro, K., DiStefano, E., Barry, J., Chen, W., Izenson, M., Possamai, F., Zimmermann, A., 2006. Small scale refrigeration system for electronic cooling within a notebook computer. ITHERM 2006, 0-7803-9524, pp. 751–758.

Moran, M.J., Shapiro, H.N., 2004. Fundamentals of Engineering Thermodynamics. John Wiley and Sons, Inc., Hoboken, NJ, USA.

Phelan, P.E., 2001. Current and future miniature refrigeration cooling technologies for high power microelectronics. Semiconductor Thermal Measurement and Management Symposium: Seventeenth Annual IEEE, San Jose, CA, pp. 158–167.

Sathe, A.A., 2008. Miniature-scale diaphragm compressor for electronics cooling, Ph.D. thesis. School of Mechanical Engineering, Purdue University, West Lafayette, USA.

Sathe, A.A., Groll, E.A., Garimella, S.V., 2008. Analytical model for an electrostatically actuated miniature diaphragm compressor. Journal of Micromechanics and Microengineering 18 (3) #035010.

Trutassanawin, S., 2006. A miniature-scale refrigeration system for electronics cooling, Ph.D. thesis. School of Mechanical Engineering, Purdue University, West Lafayette, USA.

Trutassanawin, S., Groll, E.A., Garimella, S.V., Cremaschi, L., 2006. Experimental investigation of a miniature-scale refrigeration system for electronics cooling. IEEE Transactions on Components and Packaging Technologies 29 (3), 678–687.

Yoon, J.S., 2006. Studies on the micro vapor compressor for the application to a miniature refrigeration system, Ph.D. thesis. School of Mechanical and Aerospace Engineering, Seoul National University, South Korea.